

Spatial downscaling of global climate model output for site-specific assessment of crop production and soil erosion

X.-C. Zhang*

USDA-ARS Grazinglands Research Laboratory, 7207 West Cheyenne St., El Reno, OK 73036, USA

Received 8 June 2005; accepted 15 November 2005

Abstract

Spatial and temporal mismatches between coarse resolution projections of global climate models (GCMs) and fine resolution data requirements of ecosystems models are the major obstacles for assessing the site-specific climatic impacts of climate change on natural resources and ecosystems. The objectives of this study were to: (i) develop a simple method for statistically downscaling GCM monthly output at the native GCM grid scale to station-scale using transfer functions, and (ii) further demonstrate the site-specific impact assessment of climate change on water resources, soil erosion, and crop production at Kingfisher, OK, US using the water erosion prediction project (WEPP) model. Monthly precipitation and temperature projected by the UK Hadley Centre's Climate Model (HadCM3) under the GGa emissions scenario were downloaded for the periods of 1900–1999 and 2070–2099 for the grid box containing the target station. Univariate transfer functions were derived by calibrating probability distributions of GCM-projected monthly precipitation and temperature to match those of local climatology for the 1950–1999 period. Derived functions, which were tested for 1900–1949, were used to spatially downscale the HadCM3 monthly projections of 2070–2099 to the target station. Downscaled monthly data were further disaggregated to daily weather series using a stochastic weather generator (CLIGEN) for driving the WEPP model. Disaggregated daily series preserve the monthly means and variances of precipitation and temperature of the downscaled HadCM3 output. Simulated annual runoff under the changed climate, compared with the present climate, increased by 40–48% despite the projected 5% decrease in precipitation. Simulated plant transpiration, soil evaporation, and long-term soil water reserve decreased by 5, 16.5, and 5.5%, respectively. Simulated soil loss rates were increased by some 44% under conventional tillage and doubled under conservation tillage and no-till. Simulated wheat yield increased by approximately 14% in all three tillage systems. The overall results show that the proposed downscaling technique is simple and sound, which provides an effective alternative for assessing the site-specific impacts of climate change on soil erosion and crop production. Nevertheless, the technique suffers from the same shortcomings as all other statistical downscaling methods, as it largely relies upon the accuracy of GCM projections as well as the applicability of transfer functions to future climate.

© 2005 Elsevier B.V. All rights reserved.

Keywords: Climate change; Impact assessment; Spatial downscaling; Weather generator

1. Introduction

The review of “Climate Change 2001: The Scientific Basis” prepared by the Intergovernmental Panel on Climate Change (IPCC Working Group I, 2001) has

concluded that globally averaged mean evaporation, precipitation, and rainfall intensity will very likely increase in response to increased concentrations of greenhouse gases in the atmosphere. The upward trend in total precipitation and a bias toward more intense rainfall events are of great concern for assessing the potential impacts on water resources, soil erosion, and ecosystems, because catastrophic environmental destruction is often caused by infrequent severe storms.

* Tel.: +1 405 262 5291; fax: +1 405 262 0133.

E-mail address: John.Zhang@ars.usda.gov.

Under climate changes, the potential for such projected changes to increase the risks of floods, soil erosion, and related environmental consequences is clear, but the potential damages in particular regions need to be assessed (SWCS, 2003). This information is needed for determining: (i) whether a change in soil and water management practices is warranted under climate change and (ii) what practices should be taken to adequately protect soil and water resources and to alleviate catastrophic damages if a change is warranted. Due to the interactive, integrated nature of agroecosystems, the impacts of climate change on natural resources may be best assessed using agricultural systems models such as the water erosion prediction project (WEPP) model.

The WEPP model is a physically based, continuous simulation model that simulates hydrology, daily water balance, plant growth, soil, and erosion at field, hillslope, and small watershed scales (Flanagan and Nearing, 1995). The plant growth and water balance components of the model were modified to account for the CO₂ effects on evapotranspiration and biomass production. The modified WEPP model has been used by many researchers to study the impacts of climate change on runoff and erosion (e.g., Savabi et al., 1993; Pruski and Nearing, 2002a,b; Zhang et al., 2004). Overall results from those studies indicated that a 1% increase in precipitation would result in a 0.5–4% increase in soil loss and a 1–4% increase in surface runoff. In those studies, changes in mean monthly projections at the native grid scale of global climate models (referred to as GCMs in this study) were directly incorporated into station daily weather series using a stochastic weather generator. This type of approach without explicit spatial downscaling tends to provide a first-order sensitivity of regional response to climate change (Hewitson, 2003; Zhang, 2006; Zhang and Liu, 2005).

Two major obstacles exist in assessing the site-specific impacts of climate change on natural resources of a particular field or farm. These obstacles are spatial and temporal scale mismatches between coarse resolution projections of GCMs and fine resolution data requirements of agricultural systems models (Hansen and Indeje, 2004). Both dynamic and empirical (statistical) approaches are used to bridge the spatio-temporal gaps. Dynamic downscaling is used to achieve higher spatial resolutions by nesting regional climate models (RCM) within GCM output fields. RCM output is computationally costly (Solman and Nuñez, 1999), and is only available for limited regions. Therefore, statistical methods are frequently used to downscale GCM projections to finer spatiotemporal scales.

A diverse range of statistical downscaling techniques has been developed. Those techniques in principle fall in three categories: weather generators, transfer functions, and weather typing schemes (von Storch et al., 2000; Wilby et al., 1998b). The transfer function approach involves deriving statistical relationships between observed local climatic variables (predictands) and large-scale GCM output (predictors) using regression-type methods such as multivariate linear or non-linear regressions, principal component analysis (PCA), canonical correlation analysis (CCA), Kriging, and artificial neural networks (ANN). Most commonly used predictors from GCM output include vorticity, airflow indices, wind strength and direction, mean sea-level pressure, geopotential heights at 500 and 700 hPa, and relative humidity (Wilby and Wigley, 2000; Solman and Nuñez, 1999; Wilby et al., 1998b; Sailor and Li, 1999; Trigo and Palutikof, 2001). In addition, Kilsby et al. (1998) included altitude, distance from coast, and geographical location of the target station as predictors in their regression equations.

Widmann et al. (2003) found that statistical precipitation downscaling directly using GCM precipitation as a predictor performed considerably better than conventional methods using other predictors as listed above. The successful use of precipitation as the predictor is primarily because the climate model is most likely to capture the effects of changes in the climate state on precipitation within its internal parameterization and calibration. For a similar reason, Wood et al. (2004) used GCM precipitation as the sole predictor for bias correction using quartile plots between GCM output and measured-precipitation at the same (regional) spatial scale. Overall, compared with the dynamic methods, the advantages of the statistical approaches are their easiness to implement and the ability to calibrate to local conditions (Solman and Nuñez, 1999). However, the major concern of the statistical approaches is whether statistical relationships derived based on the present climate are fully applicable to future climate.

Generation of daily weather series of future climate, which is required by many process-based agricultural systems models for impact assessment, is often achieved using stochastic weather generators. Model parameter values of future climate are developed by perturbing parameter values of the present climate under the guidance of GCM-projected relative changes (e.g., Wilks, 1992; Katz, 1996; Semenov and Porter, 1995; Semenov and Barrow, 1997; Mavromatis and Jones, 1998; Zhang et al., 2004), or are directly estimated using statistical relationships developed between model

parameters and GCM output fields (Wilby et al., 1998a; Kilsby et al., 1998).

Stochastic daily weather generators such as WGEN (Richardson and White, 1984) and CLIGEN (Nicks and Gander, 1994) have been widely used in the US to generate daily weather series from monthly GCM projections (e.g., Wilks, 1992, 1999; Katz, 1996; Hansen and Indeje, 2004; Pruski and Nearing, 2002b; Zhang et al., 2004). Model parameters of these weather generators can be readily manipulated to simulate arbitrary changes in mean and variance quantities for sensitivity analysis, or be deliberately modified to mimic changes in mean and variance as predicted by GCM for impact assessment. As stated in the SWCS (2003) report, precipitation intensity would increase at a rate greater than the rate of increases in mean. This trend toward precipitation occurring in more intense and more extreme events may be simulated through modifying mean and variance of daily precipitation distributions. A change in mean would largely result in a shift in daily precipitation distribution, but changes in variance would change the shape of the distribution, especially in the tail region, which controls the intensity and frequency of extreme events.

Zhang et al. (2004) developed a method for disaggregating GCM monthly projections to daily weather series using CLIGEN by adjusting both means and variances of precipitation and temperature. This temporal downscaling or disaggregation method has been further used in central Oklahoma (Zhang, 2006) and in the Changwu tableland region of southern Loess Plateau of China (Zhang and Liu, 2005). These studies without an explicit spatial downscaling tend to reflect more of a first-order regional sensitivity of natural resources to climate change. To simulate the site-specific impacts of climate change on natural resources and ecosystems using agricultural systems models, explicit spatial downscaling methods for deriving statistical relationships pertaining to particular locations need to be developed.

The objectives of this study are to: (i) develop a simple method for spatially downscaling GCM estimates of climate change at the native GCM grid scale to station-scale for monthly precipitation and temperature using transfer functions derived by matching probability distributions of GCM output with those of local climatology for the calibration period of 1950–1999, (ii) at the station-scale further disaggregate monthly values to daily weather series following the method of Zhang et al. (2004), and (iii) assess, as an example, the site-specific impacts of climate change on water resources, soil erosion, and crop production using the

WEPP model on the Kingfisher site, Oklahoma, US. The GCM-projected monthly precipitation and temperature for the GGA emissions scenario are temporally and spatially downscaled by considering distributions including mean and variance to generate daily weather input for driving the WEPP model.

2. Materials and methods

2.1. Climate change scenario

The climate change scenario of GGA1, projected under the GGA emissions scenario using the Hadley Centre's third generation climate model (HadCM3), was used in this study. The GGA forcing used the historical increase in the individual greenhouse gases from 1860 to 1990, and then the individual increases in greenhouse gases as described in the IS95a (a 1% per year compound rise in radiative forcing) emissions scenario. Note that the CO₂ increase in IS95a is similar to the CO₂ increase in IS92a. In this scenario, for example, the total CO₂ concentration in the atmosphere would increase by approximately 80% by year 2085. The IS92a scenario was considered benchmark and widely used in the impact studies in the past.

The HadCM3 model was configured with grid boxes that extended 2.5° by 3.75° (latitude by longitude). The grid box (between 35°N and 37.5°N and from 101.25°W to 97.5°W), containing the target station of Kingfisher, Oklahoma (35.87°N and 97.93°W), was selected. The monthly precipitation, mean maximum temperature, and mean minimum temperature that were projected for the box for the periods of 1900–1999 and 2070–2099 were extracted from the HadCM3 GGA1 output. Projected data of 1950–1999 were used as the control to develop transfer functions in conjunction with measured data of the same period, and data from 1900 to 1949 were used to test those transfer functions. Projected data from 2070 to 2099 were assumed to represent a changed climate, and were temporally and spatially downscaled to daily weather data for the Kingfisher station for impact assessment, as an example.

2.2. Spatial downscaling

The GCM-projected monthly precipitation from 1950 to 1999 (referred to as hindcast) was used as the control, and the historical monthly precipitation between 1950 and 1999 as the baseline. For each calendar month, the ranked observational monthly precipitation (*Y*-axis) was plotted with the ranked GCM-projected precipitation (i.e., paired by their ranks or

corresponding quartiles of the observed versus projected monthly precipitation, also called qq-plot). A simple univariate linear and a non-linear function were fitted to each plot to obtain transfer functions for each month using the LAB-fit Software (Universidade Federal de Campina Grande, Brazil). This curve fitting software automatically searches through about 200 non-linear functions having one independent variable and up to four fitting parameters, and produces a list of functions ranked by their residual errors.

Those transfer functions were used to downscale the 1900–1949 monthly precipitation of the GCM grid box to monthly precipitation at the Kingfisher station. The probability distributions of the downscaled monthly precipitation were compared with those of the measured monthly precipitation at the station during 1900–1999 for preliminary testing. For impact assessment, those transfer functions were further used to downscale 2070–2099 monthly precipitation at the native GCM scale to those at the Kingfisher station under the premise that the transfer functions developed under the present climate are applicable to the changed climate. For each calendar month, the non-linear function was used to transform the projected monthly precipitation values that were within the range in which the non-linear function was fitted, while the linear function was used for the values outside the range. The use of linear functions for the out-of-range values is to generate conservative, first-order approximations. The downscaled monthly precipitation values, which represent the future monthly precipitation distribution at the Kingfisher station, were then used to calculate monthly mean and variance of the changed climate for the location. Those calculated

mean and variance of the downscaled monthly precipitation were used in the temporal downscaling method of Zhang et al. (2004) to generate daily weather series of the changed climate at the Kingfisher station as presented in Section 2.3.

Likewise, the GCM-projected monthly maximum and minimum temperatures were downscaled spatially in the same manner as was for monthly precipitation. Mean temperature shifts as well as variance ratios between the downscaled monthly GCM projections of 2070–2099 and the local monthly measurements of 1950–1999 were calculated for each month and were further used in temporal downscaling. In addition, two non-parametric tests, the Wilcoxon Rank Sum and the Kolmogorov–Smirnov (K–S) tests, which are applicable to any distribution, were used to test the null hypothesis that two populations such as measured versus downscaled values are identical.

2.3. Temporal downscaling

2.3.1. Precipitation

Measured daily weather data of 1950–1999 at Kingfisher were used to estimate the baseline CLIGEN input parameters, which were subsequently adjusted for the relative changes in Table 1 to generate the changed climate scenario for the target station. Adjusted precipitation parameters (Table 2) include mean (R_d) and variance (σ_d^2) of daily precipitation depths (excluding zeros) and conditional transition probabilities of a wet day following a dry day ($P_{w/d}$) and a wet day following a wet day ($P_{w/w}$). For transition probability adjustment, linear relationships between transition probabilities and

Table 1

Mean and variance of spatially downscaled GCM monthly precipitation of 2070–2099 for Kingfisher, and shift and variance ratio calculated for the downscaled monthly temperatures of 2070–2099 vs. measured local monthly data of 1950–1999

	Month											
	January	February	March	April	May	June	July	August	September	October	November	December
Monthly precipitation												
Mean R_m (mm)	33.9	39.5	67.1	70.6	127.6	59.0	47.0	37.3	104.5	66.7	57.7	29.9
Variance σ_m^2 (mm ²)	1002	1150	2517	2297	9532	2401	799	1464	6221	2698	3155	866
Monthly maximum temperature												
Mean (°C)	14.3	16.5	21.0	25.6	29.2	36.1	38.9	38.5	33.3	27.8	19.6	12.9
Mean shift (°C)	5.25	4.26	3.92	2.82	1.94	3.82	3.53	3.62	3.16	3.64	3.60	2.39
Variance ratio ^a	0.28	0.67	0.89	1.17	0.53	0.94	1.03	0.79	1.49	1.29	0.71	0.67
Monthly minimum temperature												
Mean (°C)	0.5	2.0	7.6	12.9	17.9	25.2	26.6	26.1	21.6	15.1	9.2	1.3
Mean shift (°C)	4.32	3.23	4.70	4.16	3.74	5.96	4.88	5.21	5.05	5.11	6.25	3.38
Variance ratio	0.40	0.55	0.84	0.94	0.92	0.77	1.17	0.91	0.80	0.76	0.91	0.92

^a Ratios were calculated as 2070–2099 over 1950–1999.

Table 2
Adjusted CLIGEN input parameters for generating GGal climate scenario of 2070–2099 for Kingfisher

	Month											
	January	February	March	April	May	June	July	August	September	October	November	December
Mean R_d (mm)	6.7	7.7	8.8	9.7	12.1	8.7	7.8	7.8	13.9	11.0	10.2	7.2
Variance σ_d^2 (mm ²)	152.9	163.3	266.4	235.0	841.3	306.1	73.6	261.8	679.5	313.7	459.5	160.5
$P_{w/w}$	0.34	0.36	0.38	0.36	0.42	0.31	0.30	0.26	0.37	0.38	0.38	0.27
$P_{w/d}$	0.12	0.13	0.18	0.18	0.26	0.18	0.15	0.12	0.19	0.13	0.13	0.10
Mean T_{max} (°C)	14.3	16.5	21.0	25.6	29.2	36.1	38.9	38.5	33.3	27.8	19.6	12.9
S.D. T_{max} (°C)	3.9	6.3	6.6	6.0	3.3	3.8	3.9	3.6	6.4	6.3	5.4	5.5
Mean T_{min} (°C)	0.5	2.0	7.6	12.9	17.9	25.2	26.6	26.1	21.6	15.1	9.2	1.3
S.D. T_{min} (°C)	3.8	4.4	5.5	5.5	4.5	3.3	3.4	3.3	4.4	4.8	5.6	5.4

R_d , mean precipitation per wet day; σ_d^2 , variance of wet day precipitation; $P_{w/w}$, probability of wet day following wet day; $P_{w/d}$, probability of wet day following dry day, S.D., standard deviation, T_{max} , maximum temperature; T_{min} , minimum temperature.

mean monthly precipitation (R_m) were developed for each calendar month using historical station records. For each calendar month (say January), approximately 20–25 wettest and driest months were selected to compute $P_{w/w}$, $P_{w/d}$, and R_m for each group. Linear relationships between $P_{w/w}$ and R_m as well as between $P_{w/d}$ and R_m were then established using the two data points (one pair for wet group and another for dry group). Adjusted $P_{w/w}$ and $P_{w/d}$ for the changed climate were interpolated for the downscaled R_m of Table 1 using the linear relationships. Caution must be taken to ensure that the projected monthly mean precipitation is within the range in which the linear relationships are developed. For convenience, the adjusted conditional transition probabilities are equivalently expressed in term of an unconditional probability of daily precipitation occurrence (π) and a dependence parameter (r) defined as the lag-1 autocorrelation of daily precipitation series:

$$\pi = \frac{P_{w/d}}{1 + P_{w/d} - P_{w/w}} \quad (1)$$

$$r = P_{w/w} - P_{w/d} \quad (2)$$

The adjusted mean daily precipitation per wet day (R_d , Table 2) was estimated as:

$$R_d = \frac{R_m}{N_d \pi} \quad (3)$$

where N_d is the number of days in the month and $N_d \pi$ is the average number of wet days in the month. Since the downscaled variances of GCM monthly precipitation of 2070–2099 were available for the target station (σ_m^2 , Table 1), the adjusted daily precipitation variances (σ_d^2 , Table 2) were approximated

using Eq. (11b) of Wilks (1999) instead of the proportional method of Zhang et al. (2004) as follows:

$$\sigma_d^2 = \frac{\sigma_m^2}{N_d \pi} - \frac{(1 - \pi)(1 + r)}{1 - r} R_d^2 \quad (4)$$

All adjusted precipitation parameter values were input to CLIGEN to generate 100 years of daily precipitation for preliminary tests. The generated average annual precipitation was approximately 8% greater than the downscaled target annual average. Thus, to match the target precipitation, the initially adjusted mean daily precipitation using Eq. (3) was scaled down by 8% for each of the 12 calendar months, and the results are given in the first row of Table 2. The overestimation might have resulted from a combined effect of a general increase in daily precipitation variance in the changed climate and a skewed (or transformed) normal distribution of daily precipitation employed in CLIGEN, as well as model approximation errors.

2.3.2. Maximum and minimum temperature

Downscaled monthly temperature means and temperature variance ratios between spatially downscaled monthly projections of 2070–2099 and measured monthly values of 1950–1999 were calculated for each calendar month (Table 1). Downscaled mean maximum and minimum temperatures were directly used in CLIGEN as the adjusted monthly means for the changed climate (Table 2). Adjusted daily temperature variances were obtained by multiplying the baseline daily temperature variances by the calculated variance ratios of Table 1 for each month. This method is appropriate if autocorrelation coefficients of all orders in the baseline climate are similar to those in the downscaled future climate (Katz, 1985). All new parameter values (Table 2) were input to CLIGEN, and 100 years of daily weather

data of the GGal climate scenario of 2070–2099 were generated for Kingfisher.

2.4. WEPP model calibration

Three experimental watersheds, located at the US Department of Agriculture, Agricultural Research Service, Grazinglands Research Laboratory, 7 km west of El Reno, Oklahoma were used in model calibration. The watersheds are 80 m wide and 200 m long with a drainage area of 1.6 ha each. The longitudinal slope of the watersheds is approximately 3–4%. Soils (fine, mixed, thermic, Udertic Paleustoll) are predominantly silt loam with an average of 23% sand and 56% silt in the tillage layer. The watersheds were in the annual winter wheat-summer fallow rotation in contrasting management and tillage systems including conventional tillage, conservation tillage, and no-till from 1980 to 1995. Precipitation, surface runoff, and sediment were recorded between 1985 and 1995, and wheat yields and soil moisture contents were intermittently measured during the period.

The hydrology, water balance, and plant growth components were calibrated using the above measured hydrological and winter wheat data on these watersheds. The calibrated WEPP model simulated annual surface runoff and wheat above ground biomass at harvest relatively well (Zhang, 2004). Specifically, the model efficiency, which is a good measure of model prediction relative to measured data, between WEPP-predicted and measured annual runoff was 0.31 on the conservation tillage watershed. The model efficiency between predicted and measured above ground biomass at harvest was 0.50.

In this study, the WEPP erosion component was further calibrated on the three watersheds using measured sediment data. Since soil properties in the three watersheds are similar, one set of the erodibility parameters (interrill erodibility, rill erodibility, and rill critical shear stress) is calibrated. These three parameters were adjusted to minimize the differences between measured and simulated average annual soil losses for each of the three watersheds under contrasting tillage. Since the proportion of interrill to rill erosion normally vary with tillage systems such as no-till versus conventional tillage, the estimated soil erodibilities should be more dependable than those when only one tillage system was used in calibration. The measured and calibrated average annual soil losses at the El Reno site were 5712 and 5600 kg/ha, respectively, for the conventional tillage watershed, 2262 and 2464 kg/ha for the conservation tillage watershed, and 269 and 672 kg/ha for the no-till watershed. The

good agreement indicates that the relative effects of crop management including tillage operations on soil erosion are adequately represented in WEPP.

The WEPP model (Version 2004.7), which was modified to be CO₂-sensitive, was used in the simulation. The modified WEPP model as described by Favis-Mortlock and Savabi (1996) automatically invokes CO₂-sensitive biomass production and plant transpiration subroutines when CO₂ concentration is above the present level.

2.5. Simulated management systems under future climate

Four input files (i.e., slope, soil, climate, and crop management) are needed to run the WEPP model. Measured slope profile, soil properties, as well as calibrated crop and soil erodibility parameters were used to build the slope and soil input files. A common regional cropping system (annual winter wheat-summer fallow) and three contrasting tillage systems (conventional, conservation, and no-till) were used. For the simulations under the present climate, winter wheat was planted on October 15 and harvested on June 15 of the following year. However, for the simulations of the future climate (2070–2099), a new planting date of November 1 and a harvest date of June 1, which are representative of northern Texas where the present temperature regime is similar to the projected temperature in central Oklahoma, were used to accommodate the elevated temperature. For tillage operations, one moldboard plow and three disk operations, approximately 1 month apart in the summer, were used in the conventional tillage treatment. In contrast, three disk operations, which left about 50% of residue on the soil surface for each operation, were used in the conservation tillage treatment. The WEPP model was run for 100 years for the three tillage systems under the present and future climates of Kingfisher using the slope and soil input files of El Reno. The simulation was conducted as if the El Reno watershed were relocated to the Kingfisher station, which is about 40 km north of El Reno. Simulated surface hydrology, soil erosion, and wheat production under the changed climate were compared to those under the present climate.

3. Results and discussion

3.1. Spatial downscaling of monthly precipitation

Linear and non-linear univariate regressions between the corresponding quartiles of monthly precipitation depths at the native GCM grid box versus those

Table 3
Determination coefficients (r^2) of linear and non-linear univariate regressions between measured at Kingfisher vs. GCM-projected monthly values for the grid box for the period of 1950–1999

Month	Precipitation		Maximum temperature		Minimum temperature	
	Linear	Non-linear	Linear	Non-linear	Linear	Non-linear
January	0.975	0.989	0.953	0.967	0.835	0.972
February	0.932	0.969	0.968	0.984	0.841	0.961
March	0.917	0.996	0.963	0.965	0.954	0.980
April	0.969	0.980	0.983	0.986	0.944	0.980
May	0.971	0.992	0.891	0.967	0.969	0.990
June	0.971	0.987	0.942	0.990	0.847	0.942
July	0.905	0.963	0.957	0.997	0.785	0.991
August	0.935	0.967	0.936	0.986	0.702	0.927
September	0.987	0.990	0.952	0.965	0.728	0.988
October	0.921	0.987	0.933	0.951	0.816	0.987
November	0.951	0.951	0.951	0.955	0.847	0.945
December	0.948	0.988	0.896	0.975	0.890	0.978

measured at Kingfisher were carried out for each month for the period of 1950–1999. The determination coefficients (r^2) of linear regressions ranged from 0.905 for July to 0.987 for September, and those of non-linear regressions from 0.951 for November to 0.996 for March, indicating that either linear or non-linear functions will do a good job in reproducing measured probability distributions (Table 3). A qq-plot is illustrated in Fig. 1a, with July being the least linear, September the most, and March an ‘S’ shape. Fig. 1a also illustrates that the raw GCM projections for the grid box were consistently greater than the corresponding

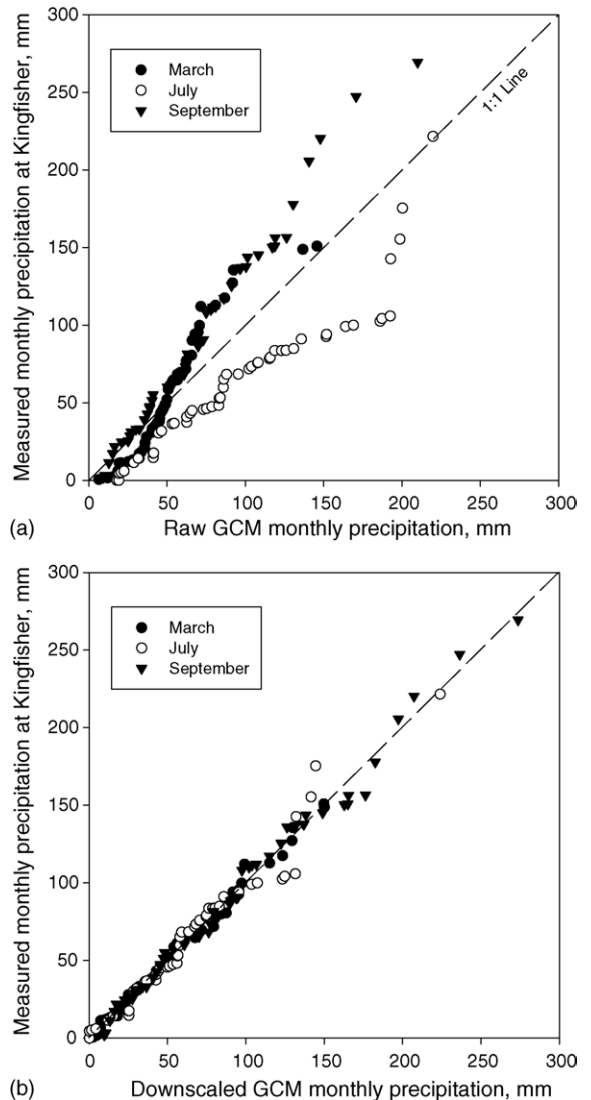


Fig. 1. (a and b) qq-Plots of monthly precipitation depths measured at Kingfisher vs. those projected by HadCM3 for the native grid box for the period of 1950–1999 for March, July, and September. Note that values are paired by their ranks within respective data series.

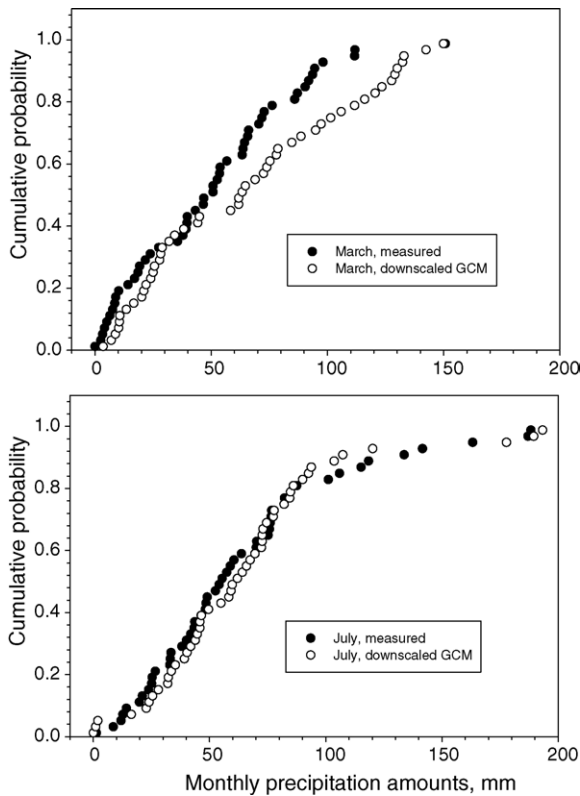


Fig. 2. Cumulative probability distributions of measured and spatially downscaled GCM monthly precipitation for the period of 1900–1949 for March and July.

measured monthly precipitation at Kingfisher for July and consistently less for September, showing an overall overprediction for the former and underprediction for

the latter. However for March, drier months were overpredicted while wetter months were underpredicted. Fig. 1b shows the qq-plot for the downscaled GCM monthly precipitation of 1950–1999 using non-linear transfer functions for the 3 months, indicating how well the transfer functions reproduced the probability distributions of measured monthly precipitation, as was also evidenced by the great r^2 values.

Probability distributions of the downscaled GCM monthly precipitation and measured monthly precipitation for the period of 1900–1949 are shown in Fig. 2 for March and July. July illustrates a good match while March is a poor match, as was also reflected in Table 4. There were no statistical differences between the two distributions at $P = 0.05$ for the Wilcoxon and K–S tests, while there were two significant differences for March and April at $P = 0.1$ for the Wilcoxon tests. The critical significance probability levels (P) in Table 4 are the probabilities of being wrong if we reject the null hypothesis (the two distributions are identical) that is actually true. Thus, the greater the critical probability levels, the less confidence or evidence we have for rejecting the null hypothesis. All P values between the measured and spatially downscaled monthly precipitation for the period of 1950–1999 were greater than 0.5 (Table 4), among which 15 were greater than 0.95, indicating that the transfer functions reproduced the measured distributions well. The absence of significant differences in monthly precipitation distributions between the first (1900–1949) and second half (1950–1999) of the century at $P = 0.1$, for either observations or downscaled GCM projections, suggest

Table 4

Critical significance probability levels of the Wilcoxon rank sum and Kolmogorov–Smirnov (K–S) tests for measured monthly precipitation at Kingfisher and GCM-monthly precipitation downscaled to Kingfisher using transfer functions (both tests test for difference between the two distributions)

	Month											
	January	February	March	April	May	June	July	August	September	October	November	December
Measured 1900–1949 vs. measured 1950–1999												
Wilcoxon ^a	0.436	0.699	0.617	0.129	0.333	0.888	0.888	0.890	0.132	0.347	0.759	0.839
K–S	0.711	0.864	0.864	0.393	0.393	0.964	0.964	0.964	0.544	0.544	0.711	0.544
Downscaled GCM 1900–1949 vs. downscaled GCM 1950–1999												
Wilcoxon	0.295	0.866	0.288	0.973	0.707	0.356	0.945	0.931	0.644	0.152	0.515	0.191
K–S	0.711	0.711	0.393	0.964	0.393	0.270	0.964	0.393	0.864	0.178	0.178	0.711
Measured 1900–1949 vs. downscaled GCM 1900–1949												
Wilcoxon	0.321	0.579	0.080	0.081	0.493	0.156	0.702	0.785	0.211	0.712	0.285	0.145
K–S	0.864	0.393	0.178	0.393	0.178	0.270	0.964	0.864	0.393	0.711	0.544	0.112
Measured 1950–1999 vs. downscaled GCM 1950–1999												
Wilcoxon	0.540	0.728	0.975	0.970	0.964	0.764	0.931	0.959	0.962	0.964	0.931	0.942
K–S	0.711	0.711	1.000	1.000	0.997	0.964	0.997	0.864	0.997	0.997	0.964	0.997

^a Two sided test with normal approximation.

that the precipitation at Kingfisher has been reasonably stationary. The comparable P levels between measured and downscaled precipitation over the century mirror the similarity of probability distributions of the two. When downscaling the GCM monthly precipitation of 1900–1949 using the transfer functions, 12 data points (1, 2, 2, 3, 3, and 1 for January, February, June, July, November, and December, respectively) were outside the ranges, and were downscaled using the linear functions instead.

For impact assessment, the GCM monthly precipitation of 2070–2099 was downscaled to the Kingfisher station using the fitted transfer functions. Eight data points (2, 2, 1, and 3 for January, May, September, and November, respectively) were outside the ranges, and were downscaled using the linear functions. Probability distributions of downscaled GCM monthly precipitation for the 2070–2099 period and those of measured monthly precipitation for the 1950–1999 period are shown in Fig. 3 for March and July as an example. Compared with the baseline climate, downscaled precipitation of 2070–2099 would increase by 21% for March and decrease by 27% for July. In general, downscaled mean monthly precipitation would decrease in summer (June, July, and August) but increase in the remaining months except December. Changes of precipitation variances followed a similar seasonal pattern of changes in monthly mean precipitation.

3.2. Spatial downscaling of monthly mean temperature

The regression r^2 between measured and raw GCM monthly mean maximum temperature (T_{\max}) for the 1950–1999 period for any of the 12 months was greater than 0.89 for linear regressions and 0.95 for non-linear regressions (Table 3). However for minimum temperature (T_{\min}), it was greater than 0.70 for linear regressions and 0.92 for non-linear regressions. Univariate linear functions fitted ranked monthly mean temperature better for T_{\max} than for T_{\min} for all months except May, and non-linear functions consistently outperformed linear functions for all 12 months for both T_{\max} and T_{\min} . The better fits of non-linear transfer functions encourage their use in downscaling the data points within the ranges in which the regression equations were fitted. However, for the data points outside the ranges, linear functions were used for reliable estimates. A qq-plot of T_{\max} is illustrated in Fig. 4a for January (winter) and August (summer). HadCM3 consistently underpredicted the correspond-

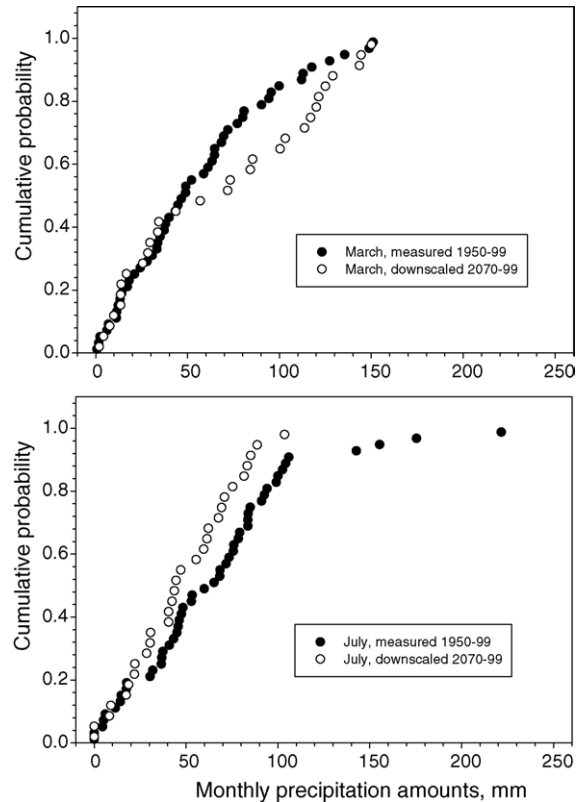


Fig. 3. Cumulative probability distributions of measured monthly precipitation during 1950–1999 and spatially downscaled GCM monthly precipitation for the period of 2070–2099.

ing quartiles of monthly mean T_{\max} for January, and underpredicted T_{\max} for cooler months but overpredicted for warmer months of August, as compared to the measured T_{\max} for the 1950–1999 period. The downscaled GCM T_{\max} values are plotted in Fig. 4b for January and August, illustrating how well the non-linear functions reproduced the probability distributions of the measured T_{\max} . In general, the measured probability distributions were well reproduced by the transfer functions for both T_{\max} (Table 5) and T_{\min} (Table 6) for the period of 1950–1999.

Probability distributions of downscaled GCM monthly mean T_{\max} were shifted to smaller values considerably for January and slightly for July, as compared to those of measured T_{\max} in Fig. 5 for the period of 1900–1949, indicating an underestimation of downscaled GCM T_{\max} for both months. January illustrates a typical ‘poor’ match between the measured and downscaled GCM distributions for the period (Table 5), while July reflects a typical ‘good’ match among the 12 months. The Wilcoxon and K–S tests show that the distributions are statistically different at

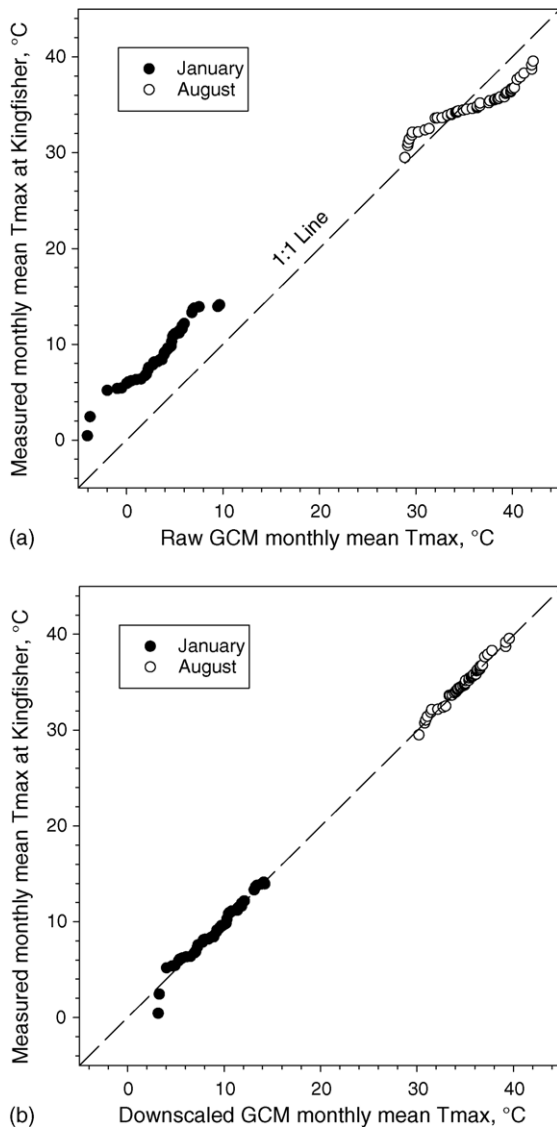


Fig. 4. (a and b) qq-Plots of monthly mean maximum temperature (T_{max}) measured at Kingfisher vs. those projected by GCM for the native grid box for 1950–1999 for January and August. Note that values are paired by their ranks within respective data series.

$P = 0.05$ for 8 out of 12 months for both T_{max} (Table 5) and T_{min} (Table 6) for the period of 1900–1949. Such significant differences were most likely caused by transient bias in the GCM integration rather than transfer functions. This bias likely results from internal stochastic inter-decadal variability in the climate model. While such variability, which constitutes a large portion of the observed 20th Century trends, may be realistic, there is no expectation that it will match the observed inter-decadal variability since it is not related to external forcing. This type of bias may be balanced out if

multiple ensemble simulations or climate models are used in aggregate.

There were no significant differences in measured distributions between 1900–1949 and 1950–1999 for the Wilcoxon and K–S tests at $P = 0.05$ for both T_{max} and T_{min} for all 12 months except for T_{max} of September. However, downscaled GCM distributions of 1900–1949 were different from those of 1950–1999 at $P = 0.05$ for T_{min} for 7 out of 12 months for both tests (Table 6), and for T_{max} for 6 out of 12 for the Wilcoxon test and for 3 out of 12 for the K–S test (Table 5). The contrasting results between measured and downscaled GCM distributions over the century indicated that there was a non-stationary bias in the GCM integration during the 1900–1999 period as discussed above. Note that a stationary bias or a systematic error would be filtered out by those transfer functions. The non-stationary bias was that HadCM3-projected mean temperature increased at a rate greater than the observed rate at Kingfisher during 1900–1999. This bias was also contributed to the differences between measured and downscaled GCM distributions of 1900–1949. As discussed in Section 1, all statistical downscaling techniques are based on the premise that GCM output is accurate (e.g., Wilby et al., 1998a; Wilby and Wigley, 2000; von Storch et al., 2000). This simple downscaling method is unable to correct any non-stationary bias in the GCM output. It should be mentioned that when downscaling the 1900–1949 GCM temperatures, three data points per calendar month, on an average, for T_{max} and two for T_{min} were outside the ranges, and were downscaled using the linear functions.

The monthly mean T_{max} and T_{min} projected for the 2070–2099 period were downscaled to the Kingfisher station using the fitted transfer functions. On an average, 8 data points per calendar month for T_{max} and 15 for T_{min} were above the ranges and were downscaled using linear functions. Probability distributions of downscaled GCM monthly mean T_{max} for the 2070–2099 period and those of measured monthly mean T_{max} for the 1950–1999 period are shown in Fig. 6 for January and August as an example. Compared with the baseline climate, downscaled T_{max} of 2070–2099 consistently shifted to higher values for both months, with a mean increase of 5.25 °C for January and 3.62 °C for August. In general, the downscaled T_{max} shifts were greater in the winter season than in the others, with a mean annual increase being 3.50 °C (Table 1). The variance ratios were less than 1 except for April, July, September, and October, indicating an overall decrease in variance. The downscaled T_{min} shifts were greater in June thru November than in the remaining period, with

Table 5

Critical significance probability levels of the Wilcoxon rank sum and Kolmogorov–Smirnov (K–S) tests for measured monthly maximum temperature at Kingfisher and GCM-monthly maximum temperature downscaled to Kingfisher using transfer functions

	Month											
	January	February	March	April	May	June	July	August	September	October	November	December
Measured 1900–1949 vs. measured 1950–1999												
Wilcoxon ^a	0.155	0.880	0.100	0.720	0.570	0.973	0.530	0.056	0.014*	0.187	0.053	0.730
K–S	0.270	0.864	0.178	0.864	0.864	0.864	0.544	0.068	0.040*	0.178	0.068	0.544
Downscaled GCM 1900–1949 vs. downscaled GCM 1950–1999												
Wilcoxon	0.009*	0.042*	0.029*	0.007*	0.004*	0.099	0.292	0.248	0.314	0.060	0.046*	0.152
K–S	0.012*	0.112	0.178	0.040*	0.003*	0.270	0.544	0.393	0.544	0.178	0.178	0.393
Measured 1900–1949 vs. downscaled GCM 1900–1949												
Wilcoxon	0.001*	0.059	0.001*	0.001*	0.019*	0.101	0.059	0.006*	0.001*	0.002*	0.001*	0.075
K–S	0.001*	0.112	0.012*	0.006*	0.040*	0.178	0.270	0.006*	0.006*	0.006*	0.002*	0.068
Measured 1950–1999 vs. downscaled GCM 1950–1999												
Wilcoxon	0.984	0.984	0.861	0.912	0.956	0.940	0.956	0.923	0.942	0.995	0.992	0.890
K–S	0.997	1.000	0.964	0.711	0.711	0.864	0.997	0.997	0.864	0.544	0.544	0.964

^a Two sided test with normal approximation.

* Significant difference at $P < 0.05$.

a mean annual increase of 4.67 °C (Table 1). The monthly variance ratios were less than 1 except July.

The mean monthly variance ratios calculated using the downscaled GCM values of 2070–2099 and the measured data of 1950–1999 were 0.87 for T_{\max} and 0.82 for T_{\min} (Table 1). The mean variance ratios calculated using the downscaled GCM data of 2070–2099 and 1950–1999 were 0.90 for T_{\max} and 0.85 for T_{\min} , while those calculated using the raw GCM grid data of 2070–2099 and 1950–1999 were 0.94 and 0.87, respectively. In general, these variance ratios from these three methods were quite similar. However, the variance

ratios calculated using the downscaled GCM data of 1950–1999 (denominator) were approximately 1–4% greater than those calculated using the measured data of 1950–1999. This is because the curve fitting (transfer function) smoothed the measured distributions of mean monthly temperatures. The use of the measured data of 1950–1999 assumes a perfect fit, i.e., $r^2 = 1$. Since the r^2 values of the non-linear fits are close to 1 for most months, the differences between the two are very small. Actually, either one can be used in the temporal downscaling process. The use of the measured data as was done in this paper stresses the facts that those data

Table 6

Critical significance probability levels of the Wilcoxon rank sum and Kolmogorov–Smirnov (K–S) tests for measured monthly minimum temperature at Kingfisher and GCM-monthly minimum temperature downscaled to Kingfisher using transfer functions

	Month											
	January	February	March	April	May	June	July	August	September	October	November	December
Measured 1900–1949 vs. measured 1950–1999												
Wilcoxon ^a	0.182	0.572	0.926	0.533	0.558	0.893	0.228	0.314	0.381	0.828	0.804	0.904
K–S	0.270	0.544	0.964	0.178	0.393	0.864	0.393	0.393	0.544	0.864	0.997	0.997
Downscaled GCM 1900–1949 vs. downscaled GCM 1950–1999												
Wilcoxon	0.095	0.108	0.200	0.006*	0.001*	0.001*	0.058	0.010*	0.005*	0.003*	0.001*	0.203
K–S	0.178	0.068	0.270	0.022*	0.022*	0.012*	0.068	0.022*	0.022*	0.040*	0.006*	0.270
Measured 1900–1949 vs. downscaled GCM 1900–1949												
Wilcoxon	0.011*	0.196	0.133	0.001*	0.003*	0.001*	0.379	0.001*	0.001*	0.001*	0.001*	0.154
K–S	0.040*	0.040*	0.393	0.002*	0.002*	0.003*	0.068	0.001*	0.001*	0.003*	0.006*	0.544
Measured 1950–1999 vs. downscaled GCM 1950–1999												
Wilcoxon	1.000	0.888	0.992	0.907	0.978	0.931	0.926	0.882	0.975	0.970	0.992	0.858
K–S	0.997	0.544	0.997	0.964	1.000	0.711	0.864	0.711	0.964	0.997	0.864	0.964

^a Two sided test with normal approximation.

* Denotes significant difference at $P < 0.05$.

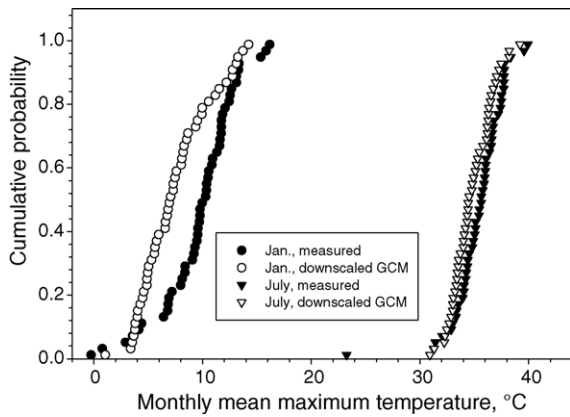


Fig. 5. Cumulative probability distributions of measured and spatially downscaled monthly mean maximum temperature (T_{\max}) for the period of 1900–1949 for January and August.

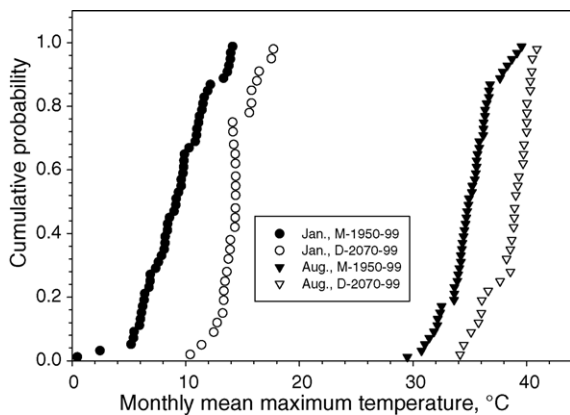


Fig. 6. Cumulative probability distributions of monthly mean maximum temperature (T_{\max}) measured (M) during 1950–1999 vs. those of downscaled (D) GCM of 2070–2099 for January and August.

were used to derive the baseline climate parameters and the calculated variance ratios were used to modify those parameters to generate the changed climate. The small differences in variance are expected to have little impact on simulated responses of runoff, soil loss, and wheat yield to climate change.

3.3. Temporal downscaling of monthly precipitation and temperature

The adjusted CLIGEN input parameters (Table 2), which were derived from the data in Table 1, were used to generate the changed climate of 2070–2099 for the Kingfisher station. The generated daily weather series for the 2070–2099 period would reflect the relative changes of Table 1 as compared to the present climate. The disaggregated daily weather series would preserve the changes of the monthly means and variances of Table 1 for both precipitation and temperature (Zhang et al., 2004). Specifically, mean monthly precipitation depths would increase in most months except June, July, and August. Averaged monthly variance of daily precipitation of the changed climate would be 64% greater than that of the baseline climate. Mean annual temperature increases would be 3.50 °C for T_{\max} and 4.67 °C for T_{\min} . Temperature variances would decrease for most months for both T_{\max} and T_{\min} .

3.4. Impact assessment

The average annual precipitation at the location under the present (baseline) climate conditions was 782 mm, and that of the downscaled GCM-projections for the 2070–2099 period was 745 mm, showing an approximately 5% decrease in annual precipitation. Despite the projected decrease in precipitation, simulated surface runoff increased 40–48% under the changed climate in

Table 7

WEPP-simulated average-annual surface runoff, plant transpiration (E_p), soil evaporation (E_s), deep percolation (D_p), mean soil water reserve in the 1.4-m profile (S_w), soil loss rate, wheat grain yield for the present and changed climates in three tillage systems for Kingfisher

Variable	Variable						
	Runoff (mm)	E_p (mm)	E_s (mm)	D_p (mm)	S_w (mm)	Soil loss (kg/ha)	Yield (kg/ha)
Present (baseline) climate, CO ₂ = 350 ppmv, precipitation = 782 mm/year							
Conventional	77	465	233	7.0	323	5152	2220
Conservation	67	465	245	5.4	320	448	2200
No-till	67	453	260	3.5	314	224	2120
Changed (2070–2099) climate of GGA1, CO ₂ = 640 ppmv, precipitation = 745 mm/year							
Conventional	108	441	194	2.4	305	7392	2510
Conservation	99	439	206	1.7	302	896	2490
No-till	97	433	215	1.2	298	448	2440

Lateral flow in soil was less than 0.03 mm/year in all simulations.

the three tillage systems as compared to the corresponding tillage systems under the present climate (Table 7). The increase in runoff was mainly caused by the overall increase in precipitation variability. As mentioned in the preceding section, overall variance of downscaled daily precipitation of the changed climate was increased by some 64% as compared with the variance of the baseline climate. An increase in precipitation variability would lead to an increase in occurrence of heavy storms, which would produce more surface runoff (Zhang et al., 2004). As a combined effect of the runoff increase and precipitation decrease, the simulated average annual plant transpiration and soil evaporation in all three tillage systems decreased by some 5 and 16.5%, respectively. The lesser decrease in plant transpiration was because of the slight increase in precipitation during the growing season of winter wheat. Likewise, the greater reduction in soil evaporation was attributed to the considerable decrease in precipitation during the fallow period, especially from June to August. The simulated deep water percolation decreased from about 5 mm per year under the present climate to 2 mm under the changed climate. The simulated long-term daily soil moisture reserve in the 1.4 m soil profile decreased by some 5.5% in all tillage systems. The reduction in percolation and soil moisture reserve was mainly attributed to the decrease in precipitation and increase in runoff, and was probably compounded by better crop growth.

Simulated wheat grain yield increased by about 14% under the changed climate (Table 7). The yield increase was an integrated result of: (i) a slight increase in precipitation during the growing season, (ii) an 80% increase in CO₂ concentration, and (iii) a moderate increase in temperature. Simulated soil losses under the changed climate, compared with the present climate, increased by 44% under the conventional tillage, and doubled under the conservation tillage and no-till due to the increases in runoff depths. However, the average annual soil losses under the changed climate were less than 900 kg/ha under the conservation tillage and no-till, indicating that these tillage systems would be sufficient in controlling soil erosion under the changed climate.

3.5. *Caveat and implications of the proposed approach*

The crux of this simple spatial downscaling method is its emphasis on reproducing probability distributions of local observations rather than searching for and building strong relationships between local variables (predictands) and GCM output variables (predictors) using

complex statistical methods such as ANN, PCA, and CCA. This simple method directly calibrates GCM monthly hindcast to probability distribution of observed data while disregarding the 1:1 correspondence between the two. This is in sharp contrast to the conventional statistical downscaling methods in literature, which are entirely built upon the existence of strong relationships between observed local variables and GCM output variables (e.g., Wilby et al., 1998b; Wilby and Wigley, 2000; Solman and Nuñez, 1999). The justification for taking this simple approach is that the impacts of a certain climate on natural resources and ecosystems can be adequately assessed under any climate scenario statistically similar or identical to the climate in consideration. The proposed method guarantees that transformed GCM hindcast reproduces probability distributions of observed data at the station-scale (i.e., ensure statistical equality), while relaxing the demands upon the existence of strong relationships between predictands and predictors. For similar reasons, Wood et al. (2004) have used qq-plots to correct GCM climatology using observed climatology at the same spatial scales.

As reviewed in Section 1, two groups of predictors have been traditionally used in the statistical downscaling. One group includes variables from GCM output, and another local physiographic variables. The proposed method assumes that the key processes and variables that affect GCM-projected precipitation and temperature have been adequately simulated during the GCM integration, and thus it is unnecessary to reconsider them during the downscaling process. This assumption is consistent with the findings of Widmann et al. (2003), who have reported that GCM-projected precipitation was a good predictor for downscaling regional precipitation. On the other hand, the calibration of GCM output directly to the target station is intended to account for the effects of local physiographic features such as elevation, land–water distribution, land use, and land surface properties on local climate, which are not considered in GCMs. Nevertheless, this approach assumes, as all statistical downscaling methods do, that GCM projections are skillful and transfer functions developed under the present climate are applicable to future climate (e.g., Wilby and Wigley, 2000; Solman and Nuñez, 1999; Busuic et al., 1999; von Storch et al., 2000).

4. Conclusions

Linear and non-linear univariate functions fit the corresponding quartiles of the monthly precipitation and temperature projected at the native GCM grid scale

and those measured at the target station well. The measured and downscaled probability distributions using the fitted transfer functions were quite similar for the 1950–1999 period for both precipitation and temperature, with the significant probability levels being close to 1 for most months for the Wilcoxon and K–S tests. The determination coefficients (r^2) of linear regressions were greater than 0.91 for precipitation, 0.89 for T_{\max} , and 0.70 for T_{\min} for all 12 months; and those of nonlinear regressions were greater than 0.95, 0.95, and 0.92, respectively. In general, non-linear functions fit better and should be used to downscale data points inside the ranges in which the transfer functions are fitted. However, for data points falling outside the ranges, linear functions should be used for conservative estimation. A considerable number of data points of T_{\max} and T_{\min} fell outside (above) the ranges when downscaling the GCM projections of 2070–2099 in this study. This result suggests that the proposed method is better suited to assess the climatic impacts of the next 20–30 years, simply because (i) lesser temperature rise in the nearer future will lead to fewer outliers and (ii) it is less likely to violate the assumption that transfer functions fitted under the present climate are applicable to future climate.

The average annual precipitation of downscaled GCM-projections for the 2070–2099 period was 742 mm, showing an approximately 5% decrease compared with the present climate. Despite the projected decrease in precipitation, simulated annual surface runoff increased 40–48% under the changed climate in all three tillage systems, resulting from an overall 64% increase in daily precipitation variance. Consequently, simulated annual plant transpiration, soil evaporation, and long-term soil moisture balance in all three tillage systems decreased. Due to the runoff increase, simulated annual soil loss was increased by about 44% under the conventional tillage. Though simulated soil losses under the conservation tillage and no-till were doubled, the absolute amounts were fairly small, suggesting these tillage systems would be sufficient to keep soil erosion low under the changed climate. Simulated wheat yield increased by some 14%, resulting from a slight increase in precipitation during the growing season, an 80% increase in CO_2 concentration, and a moderate increase in temperature. It should be reiterated that the impact assessment in this work is mainly for demonstration purpose, and more comprehensive assessment should be conducted using multiple climate models and emissions scenarios.

The overall results show that the proposed method is simple to use and viable for downscaling GCM-

projections for site-specific impact assessment. The approach emphasizes the parity of probability distributions between measured monthly quantities and downscaled GCM-projections while it relaxes the prerequisite of strong correlations between local measurements (predictands) and GCM output (predictors). The justification for taking this approach is that the impacts of a certain stationary climate on natural resources and ecosystems can be adequately assessed under any climate scenario similar or statistically identical to the climate under consideration. As one of the statistical downscaling techniques, the method is also built upon the assumption that GCMs are skillful and transfer functions derived under the present climate are applicable to future climate.

Acknowledgements

The GCM data were supplied by the Climate Impacts LINK Project (DEFRA Contract EPG I/I/I24) on behalf of the Hadley Centre and UK Meteorological Office. This work was partially supported by the Outstanding Overseas Chinese Scholars Fund of Chinese Academy of Sciences (No. 2005-2-3) and a grant of National Natural Science Foundation of China (No. 90202011). The author would also like to thank two anonymous reviewers for their valuable comments and suggestions.

References

- Busuioc, A., von Storch, H., Schnur, R., 1999. Verification of GCM-generated regional seasonal precipitation for current climate and of statistical downscaling estimates under changing climate conditions. *J. Climate* 12, 258–272.
- Favis-Mortlock, D.T., Savabi, M.R., 1996. Shifts in rates and spatial distribution of soil erosion and deposition under climate change. In: Anderson, M.G., Brooks, S.M. (Eds.), *Advances in Hillslope Processes*. John Wiley, New York, pp. 529–560.
- Flanagan, D.C., Nearing, M.A. (Eds.), 1995. *USDA-Water Erosion Prediction Project: Hillslope Profile and Watershed Model Documentation*. NSERL Report No. 10. West Lafayette, Ind.: USDA-ARS Nat. Soil Erosion Research Lab.
- Hansen, J.W., Indeje, M., 2004. Linking dynamic seasonal climate forecasts with crop simulation for maize yield prediction in semi-arid Kenya. *Agric. For. Meteorol.* 125, 143–157.
- Hewitson, B., 2003. Developing perturbations for climate change impact assessments. *Trans. Am. Geophys. Union*, EOS 84, 337–348.
- IPCC (Intergovernmental Panel on Climate Change), Working Group I, 2001. *Climate Change 2001: The scientific basis*. Contribution of Working Group I to the Third Assessment Report of the IPCC. Cambridge University Press, Cambridge, UK.
- Katz, R.W., 1985. Probabilistic models. In: Murphy, A.H., Katz, R.W. (Eds.), *Probability, Statistics, and Decision Making in the Atmospheric Sciences*. Westview, pp. 261–288.

- Katz, R.W., 1996. Use of conditional stochastic models to generate climate change scenarios. *Climatic Change* 32, 237–255.
- Kilsby, C.G., Cowpertwait, P.S.P., O'Connell, P.E., Jones, P.D., 1998. Predicting rainfall statistics in England and Wales using atmospheric circulation variables. *Int. J. Climatol.* 18, 523–539.
- Mavromatis, T., Jones, P.D., 1998. Comparison of climate change scenario construction methodologies for impact assessment studies. *Agric. For. Meteorol.* 91, 51–67.
- Nicks, A.D., Gander, G.A., 1994. CLIGEN: a weather generator for climate inputs to water resource and other models. In: *Proceedings of the Fifth International Conference on Computers in Agriculture*. American Society of Agricultural Engineers, St. Joseph, Michigan, pp. 3–94.
- Pruski, F.F., Nearing, M.A., 2002a. Runoff and soil-loss responses to changes in precipitation: a computer simulation study. *J. Soil Water Conserv.* 57, 7–16.
- Pruski, F.F., Nearing, M.A., 2002b. Climate-induced changes in erosion during the 21st century for eight U.S. locations. *Water Resour. Res.* 38 (art. no. 1298).
- Richardson, C., White, D.A., 1984. WGEN: a model for generating daily weather variables. U.S. Dept. Agr., Agricultural Research Service, Publ. ARS-8, p. 38.
- Sailor, D.J., Li, X., 1999. A semiempirical downscaling approach for predicting regional temperature impacts associated with climatic change. *J. Climate* 12, 103–114.
- Savabi, M.R., Arnold, J.G., Nicks, A.D., 1993. Impact of global climate change on hydrology and soil erosion: A modeling approach. In: Eckstein, Y., Zaporozec, A. (Eds.), *Proceedings of Industrial and Agricultural Impact of Environmental and Climatic Change on Global and Regional Hydrology*, Alexandria, Virginia. Water Environment Federation, pp. 3–18.
- Semenov, M.A., Barrow, E.M., 1997. Use of a stochastic weather generator in the development of climate change scenarios. *Climatic Change* 35, 397–414.
- Semenov, M.A., Porter, J.R., 1995. Climatic variability and the modeling of crop yields. *Agric. For. Meteorol.* 73, 265–283.
- Solman, S., Nuñez, M., 1999. Local estimates of global climate change: a statistical downscaling approach. *Int. J. Climatol.* 19, 835–861.
- SWCS, 2003. Conservation implications of climate change: Soil erosion and runoff from cropland. A Report from the Soil and Water Conservation Society. Soil and Water Conservation Society, Ankeny, Iowa. [http://www.swcs.org/docs/climate change-final.pdf](http://www.swcs.org/docs/climate%20change-final.pdf).
- Trigo, R.M., Palutikof, J.P., 2001. Precipitation scenario over Iberia: a comparison between direct GCM output and different downscaling techniques. *J. Climate* 14, 4422–4446.
- von Storch, H., Hewitson, B., Mearns, L., 2000. Review of empirical downscaling techniques. In: T. Iversen and B.A.K. Hioskar (Eds.), *Regional climate development under global warming*. General Technical Report no. 4. Conf. Proceedings RegClim Spring Meeting Jevnaker, Torbjornrud, Norway, May 8–9, 2000. pp. 29–46.
- Widmann, M., Bretherton, C.S., Salathe Jr., E.P., 2003. Statistical precipitation downscaling over the Northwestern United States using numerically simulated precipitation as a predictor. *J. Climate* 16, 799–816.
- Wilby, R.L., Wigley, T.M.T., 2000. Precipitation predictors for downscaling: observed and general circulation model relationships. *Int. J. Climatol.* 20, 641–661.
- Wilby, R.L., Hassan, H., Hanaki, K., 1998a. Statistical downscaling of hydrometeorological variables using general circulation model output. *J. Hydrol.* 205, 1–19.
- Wilby, R.L., Wigley, T.M.L., Conway, D., Jones, P.D., Hewitson, B.C., Main, J., Wilks, D.S., 1998b. Statistical downscaling of general circulation model output: a comparison of methods. *Water Resour. Res.* 34, 2995–3008.
- Wilks, D.S., 1992. Adapting stochastic weather generation algorithms for climate change studies. *Climatic Change* 22, 67–84.
- Wilks, D.S., 1999. Multisite downscaling of daily precipitation with a stochastic weather generator. *Climate Res.* 11, 125–136.
- Wood, A.W., Leung, L.R., Sridhar, V., Lettenmaier, D.P., 2004. Hydrologic implications of dynamical and statistical approaches to downscaling climate model outputs. *Climatic Change* 62, 189–216.
- Zhang, X.C., 2004. Calibration, refinement, and application of the WEPP model for simulating climatic impact on wheat production. *Trans. ASAE* 47, 1075–1085.
- Zhang, X.C., 2006. Spatial sensitivity of predicted soil erosion and runoff to climate change at regional scales. *J. Soil Water Conserv.*, in press.
- Zhang, X.C., Liu, W.Z., 2005. Simulating potential response of hydrology, soil erosion, and crop productivity to climate change in Changwu tableland region on the Loess Plateau of China. *Agric. For. Meteorol.* 131, 127–142.
- Zhang, X.C., Nearing, M.A., Garbrecht, J.D., Steiner, J.L., 2004. Downscaling monthly forecasts to simulate impacts of climate change on soil erosion and wheat production. *Soil Sci. Soc. Am. J.* 68, 1376–1385.